

## RESONANT PROPERTIES OF MOMENT COSSERAT CONTINUUM

M. P. Varygina,<sup>1</sup> O. V. Sadovskaya,<sup>1,2</sup> and V. M. Sadovskii<sup>1,2</sup>

UDC 539.37

*Using highly effective parallel calculations, it is shown that in a moment elastic medium, there is a resonant frequency which corresponds to the eigenfrequency of rotational motion of particles and does not depend on the size of the region studied.*

**Key words:** *elasticity, moment medium, parallel algorithm, resonant spectrum.*

**Introduction.** The mathematical model of moment Cosserat continuum [1, 2] taking into account material microstructure is designed to describe the stress–strain state of composites and granulated, powder, microfractured, and micropolar media. A fundamental distinction of this model from the classical theory of elasticity is that it implicitly contains a small linear parameter — the particle size of the material microstructure. As a consequence, to obtain correct numerical solutions, one needs to perform calculations on meshes whose sizes are matched to the value of this parameter. Dynamic problems in a three-dimensional formulation are effectively solved using parallel algorithms which allow one to distribute the computational load among a larger number of cluster nodes and considerably reduce the cell size of the computation mesh, thus increasing the accuracy of the numerical solution.

Numerical implementation of the model on multiprocessor computer systems is considered in [3, 4]. The present paper gives the results of an analysis of oscillatory processes which show that in a moment elastic medium, there is a resonant frequency which depends only on the inertial properties of particles of the microstructure and the elasticity parameters of the material.

**1. Basic Equations of the Model.** In addition to translational motion, which is characterized by velocity  $\mathbf{v}$ , the model of a moment medium considers independent rotations of particles with angular velocity  $\boldsymbol{\omega}$ , and along with the stress tensor  $\boldsymbol{\sigma}$  having asymmetric components, an asymmetric tensor moment stress  $\mathbf{m}$  is introduced. The complete system of equations of the model include the equations of motion, kinematic relations, and the generalized law of the linear theory of elasticity:

$$\begin{aligned} \rho \dot{\mathbf{v}} &= \nabla \cdot \boldsymbol{\sigma} + \rho \mathbf{g}, & j \dot{\boldsymbol{\omega}} &= \nabla \cdot \mathbf{m} - 2\boldsymbol{\sigma}^a + j\mathbf{q}, & \dot{\boldsymbol{\Lambda}} &= \nabla \mathbf{v} + \boldsymbol{\omega}, & \dot{\mathbf{M}} &= \nabla \boldsymbol{\omega}, \\ \boldsymbol{\sigma} &= \lambda(\boldsymbol{\delta} : \boldsymbol{\Lambda})\boldsymbol{\delta} + 2\mu\boldsymbol{\Lambda}^s + 2\alpha\boldsymbol{\Lambda}^a, & \mathbf{m} &= \beta(\boldsymbol{\delta} : \mathbf{M})\boldsymbol{\delta} + 2\gamma\mathbf{M}^s + 2\varepsilon\mathbf{M}^a. \end{aligned} \quad (1.1)$$

Here  $\rho$  is the density of medium,  $\mathbf{g}$  is the mass force vector,  $\mathbf{q}$  is the moment vector,  $\boldsymbol{\Lambda}$  and  $\mathbf{M}$  are the strain and curvature tensors, which in the natural state of the medium, is equal to zero,  $\boldsymbol{\delta}$  is the metric tensor,  $j$  is the inertial parameter equal to the product of the moment of inertia of a particle about the axis through its center of gravity and the numbers of particles in unit volume, and  $\lambda$ ,  $\mu$ ,  $\alpha$ ,  $\beta$ ,  $\gamma$ , and  $\varepsilon$  are the elasticity coefficients of an isotropic material. The standard notation and operations of tensor analysis are used: colon denotes double convolution, dot above symbol denotes time derivatives, the superscript “t” denotes transposition, and the superscripts “s” and “a” correspond to the symmetric and antisymmetric tensor components. The antisymmetric component, is identified (if necessary) with its corresponding vector. In particular, the equations of rotational motion include the tensor vector  $\boldsymbol{\sigma}^a = (\boldsymbol{\sigma} - \boldsymbol{\sigma}^t)/2$ . In Cartesian coordinates, the antisymmetric tensor

$$\boldsymbol{\omega} = \begin{pmatrix} 0 & -\omega_3 & \omega_2 \\ \omega_3 & 0 & -\omega_1 \\ -\omega_2 & \omega_1 & 0 \end{pmatrix}$$

is identified with the vector  $\boldsymbol{\omega}$  whose coordinates are equal to  $\omega_1$ ,  $\omega_2$ , and  $\omega_3$ .

<sup>1</sup>Institute of Computational Modeling, Siberian Division, Russian Academy of Sciences, Krasnoyarsk 660036.

<sup>2</sup>Siberian Federal University, Krasnoyarsk 660041; sadov@icm.krasn.ru. Translated from *Prikladnaya Mekhanika i Tekhnicheskaya Fizika*, Vol. 51, No. 3, pp. 126–136, May–June, 2010. Original article submitted April 9, 2009.

The symmetric component  $\dot{\mathbf{A}}^s = (\dot{\mathbf{A}} + \dot{\mathbf{A}}^t)/2$  of the tensor  $\dot{\mathbf{A}}$  is the strain rate tensor, and the antisymmetric component  $\dot{\mathbf{A}}^a = (\dot{\mathbf{A}} - \dot{\mathbf{A}}^t)/2$  characterizes the angular velocity of relative rotation of particles. The well-known formula  $\boldsymbol{\omega} = \nabla \times \mathbf{v}/2$  for the angular velocity of particles of a momentless medium follows from the equality  $\dot{\mathbf{A}}^a = 0$ .

The linear parameter of the material microstructure is estimated by the formula  $r = \sqrt{5j/(2\rho)}$ , based on the model representation of the medium as a close-packed ensemble of spherical particles of the same radius.

In the spatial case, system (1.1) includes 24 equations for 24 unknown functions and can be written in matrix form [3]

$$A\dot{U} = B^1U_{,1} + B^2U_{,2} + B^3U_{,3} + QU + G, \quad (1.2)$$

where  $U$  is a vector function composed of the velocity and angular-velocity components and asymmetric tensors of stresses and moment stress. In Cartesian coordinates, the vector function  $U$  becomes

$$U = (v_1, v_2, v_3, \sigma_{11}, \sigma_{22}, \sigma_{33}, \sigma_{23}, \sigma_{32}, \sigma_{31}, \sigma_{13}, \sigma_{12}, \sigma_{21}, \omega_1, \omega_2, \omega_3, m_{11}, m_{22}, m_{33}, m_{23}, m_{32}, m_{31}, m_{13}, m_{12}, m_{21}).$$

The vector  $G$  includes the mass forces and moments. The matrix coefficients  $A$ ,  $B^1$ ,  $B^2$ , and  $B^3$  are symmetric, and  $Q$  is antisymmetric. The matrix  $A$  is positive definite if the following conditions on the admissible parameter values are satisfied:

$$3\lambda + 2\mu > 0, \quad \mu > 0, \quad \alpha > 0, \quad 3\beta + 2\gamma > 0, \quad \gamma > 0, \quad \varepsilon > 0. \quad (1.3)$$

If conditions (1.3) are satisfied, the expression for the potential energy of elastic deformation is a positive quadratic form and system (1.2) is a Friedrichs-hyperbolic one [5]. The characteristic properties of system (1.2) are described by the equation

$$\det(cA + n_1B^1 + n_2B^2 + n_3B^3) = 0, \quad n_1^2 + n_2^2 + n_3^2 = 1,$$

which positive roots (velocities of longitudinal waves  $c_p$ , transverse waves  $c_s$ , torsional waves  $c_m$ , and waves of rotational motion  $c_\omega$ ) are equal to

$$c_p = \sqrt{\frac{\lambda + 2\mu}{\rho}}, \quad c_s = \sqrt{\frac{\mu + \alpha}{\rho}}, \quad c_m = \sqrt{\frac{\beta + 2\gamma}{j}}, \quad c_\omega = \sqrt{\frac{\gamma + \varepsilon}{j}}. \quad (1.4)$$

The complete system of the left eigenvectors is formed of the 12 vectors corresponding to the nonzero eigenvalues  $\pm c_p$ ,  $\pm c_s$ ,  $\pm c_m$ , and  $\pm c_\omega$ , among which  $\pm c_s$  and  $\pm c_\omega$  are two-fold, and 12 vectors for  $c = 0$ .

System (1.2) has generalized solutions with shock waves, which are defined by the system of strong-discontinuity equations

$$(cA + n_1B^1 + n_2B^2 + n_3B^3)[U] = 0, \quad (1.5)$$

where  $[U]$  is the jump of the solution across the wave front and  $c$  is the velocity of motion of the front along the normal vector  $\mathbf{n}$ . From system (1.5), it follows that, in a moment medium, shock waves of small amplitude can propagate only at velocities (1.4), and at the wave fronts, the scalar products of the left eigenvectors and the vector  $U$  remain continuous.

**2. One-Dimensional Motions with Plane Waves.** In the one-dimensional case where the required functions depend only on time and one of the spatial variables, for example,  $x_1$ , system (1.1) breaks up into four independent subsystems which describe:

— plane longitudinal waves:

$$\rho\dot{v}_1 = \sigma_{11,1}, \quad \dot{\sigma}_{11} = (\lambda + 2\mu)v_{1,1}, \quad \dot{\sigma}_{22} = \dot{\sigma}_{33} = \lambda v_{1,1}; \quad (2.1)$$

— torsional waves:

$$\begin{aligned} j\dot{\omega}_1 &= m_{11,1} + \sigma_{23} - \sigma_{32}, & \dot{\sigma}_{32} &= -\dot{\sigma}_{23} = 2\alpha\omega_1, \\ \dot{m}_{11} &= (\beta + 2\gamma)\omega_{1,1}, & \dot{m}_{22} &= \dot{m}_{33} = \beta\omega_{1,1}; \end{aligned} \quad (2.2)$$

— transverse waves (shear waves) with particle rotation:

$$\begin{aligned} \rho\dot{v}_2 &= \sigma_{12,1}, & \dot{\sigma}_{12} &= (\mu + \alpha)v_{2,1} - 2\alpha\omega_3, & \dot{\sigma}_{21} &= (\mu - \alpha)v_{2,1} + 2\alpha\omega_3, \\ j\dot{\omega}_3 &= m_{13,1} + \sigma_{12} - \sigma_{21}, & \dot{m}_{13} &= (\gamma + \varepsilon)\omega_{3,1}, & \dot{m}_{31} &= (\gamma - \varepsilon)\omega_{3,1}. \end{aligned} \quad (2.3)$$

One more subsystem is obtained from (2.3) by changing indices and also describes transverse waves.

The general solution of subsystem (2.1) is expressed by the d'Alembert formula, according to which longitudinal waves, as in the classical theory of elasticity, propagate at velocities  $\pm c_p$  and do not show dispersion. The subsystem of torsional waves (2.2) reduces to the telegraph equation for the angular velocity

$$\ddot{\omega}_1 = c_m^2 \omega_{1,11} - 4\alpha\omega_1/j.$$

The solution of the telegraph equation independent of  $x_1$  describes the uniform oscillatory rotation of particles of the medium with the oscillation period  $T = \pi\sqrt{j/\alpha}$ . The general solution can be represented in the form of the following integral formula, which is somewhat more complex than the d'Alembert formula:

$$\omega_1(\xi, \eta) = \int_0^\xi f'(\vartheta) J_0\left(-2\sqrt{(\xi - \vartheta)\eta}\right) d\vartheta + \int_0^\eta g'(\vartheta) J_0\left(-2\sqrt{\xi(\eta - \vartheta)}\right) d\vartheta + \left(f(0) + g(0)\right) J_0\left(-2\sqrt{\xi\eta}\right).$$

Here  $\xi, \eta = (t \pm x_1/c_m)\pi/T$  are dimensionless variables,  $J_0(z)$  is a Bessel function of the first kind of zero order, and  $f(\vartheta)$  and  $g(\vartheta)$  are arbitrary functions. Figure 1 gives a typical distribution of the angular velocity  $\omega_1$  in the interval between the fronts of two shock waves of torsion  $x_1 = \pm c_m t$ . The following dimensionless variables are used: time  $t' = \pi t/T$  and the spatial coordinate  $x'_1 = \pi x_1/(c_m T)$ . The amplitude at the wave fronts is considered constant during motion (its dimensionless value is equal to unity). Ahead of each front, the medium is in an unperturbed state. At the initial time, the solution considered has a smooth nonoscillating profile. With time, wavy rotational motion of particles with a characteristic wavelength approximately equal to  $c_m T$  is initiated at the shock-wave fronts.

In [6], numerical analysis of the equations of transverse waves (2.3) was performed using the von Neumann–Richtmyer difference scheme. The calculations were made for the problem of pulsed influence of a periodic system of  $\Lambda$ -shaped shear-stress pulses on an elastic medium. The calculation results show that, for fixed time, the angular velocity and the moment stresses are oscillating functions of characteristic wavelength  $c_s T$ . The maximum shear stress in a pulse was set equal to unity. Figure 2 gives curves of  $\omega'_3(x'_1)$  for a time  $t = 0.68$  msec and a pulse duration of 0.45 msec. In the calculations, the following elastic parameters for foam polyurethane [7] were used:  $\rho = 340$  kg/m<sup>3</sup>,  $\lambda = 416$ ,  $\mu = 104$ ,  $\alpha = 4.33$  MPa,  $\beta = -22.8$ ,  $\eta = 40$ , and  $\varepsilon = 5.3$  N. The moment of inertia of the particles, which depend on the microstructure size, was varied:  $j = 4.4 \cdot 10^{-4}$  kg/m (Fig. 2a) and  $j = 1.76 \cdot 10^{-3}$  kg/m (Fig. 2b). For the given values of the parameter  $j$ , the period of natural oscillations is equal to  $T = 31.7$  and  $63.3$   $\mu$ sec; the number of oscillations of the angular velocity varies accordingly (see Fig. 2).

**3. Resonant Spectra of Transverse Perturbations.** According to the general theory of hyperbolic systems for model (1.1), perturbations propagate at the finite velocities (1.4). Furthermore, the perturbations corresponding to transverse waves automatically generate waves of rotational motion, and vice versa, the perturbations corresponding to rotational motion, lead to the formation of transverse waves. As for torsional waves, transverse waves are also subjected to oscillations of the solution, which is the main qualitative feature which differs the Moment Cosserat model from the classical linear theory of elasticity. Another difference is that in a moment medium there is an eigenfrequency of the acoustic resonance of the material which does not depend on the sizes of the region studied and manifests itself only under certain perturbation conditions. Indeed, in the case of a homogeneous stress state, system (2.3) leads to the classical resonant equation

$$j\ddot{\omega}_3 = -4\alpha\omega_3 + 2\alpha\dot{\chi}, \quad (3.1)$$

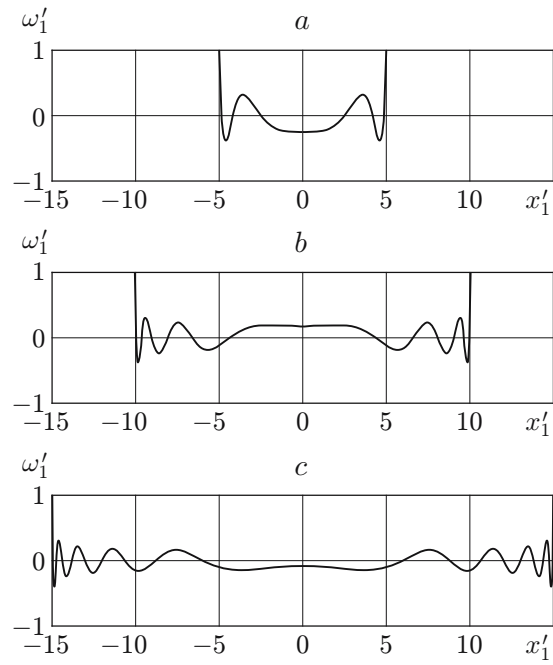


Fig. 1. Solution of the telegraph equation for various dimensionless times:  $t' = 5$  (a), 10 (b), and 15 (c).

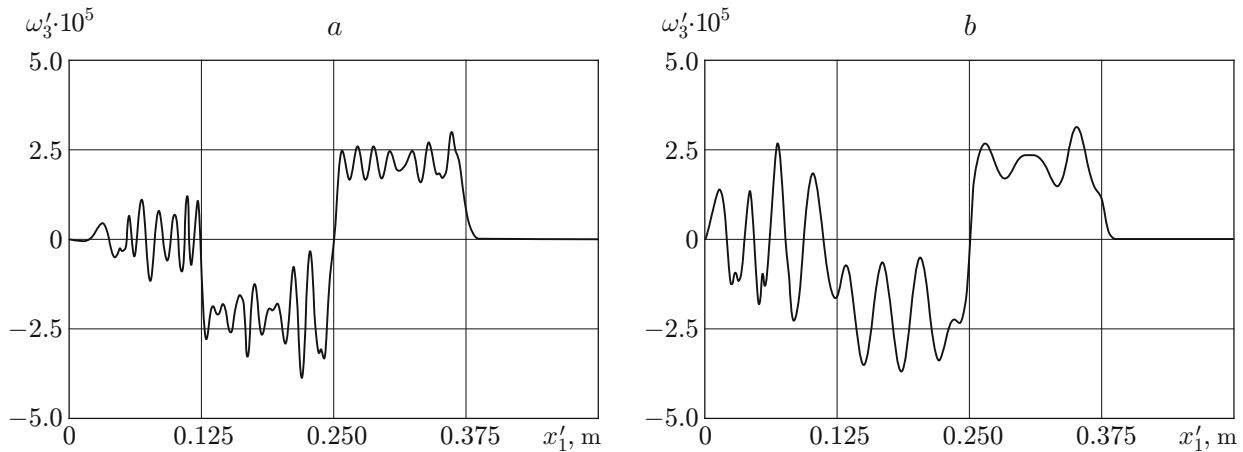


Fig. 2. Natural oscillations of the angular velocity for various particle sizes of the material microstructure: (a)  $j = 4.4 \cdot 10^{-4}$  kg/m; (b)  $j = 1.76 \cdot 10^{-3}$  kg/m.

from which it follows that, if the shear angle  $\chi(t)$  changes under a harmonic law at the frequency  $\nu_* = 1/T$  equal to frequency of natural oscillations of rotational motion, the angular-velocity amplitude of the particles increases infinitely.

Equation (3.1) describes the behavior of an infinitely thin flat elastic layer whose lower surface is motionless and the upper surface moves under a specified law. Figure 3 gives the amplitude–frequency dependences for the shear stress on the lower surface of the layer obtained by numerical solution of the problems of uniform cyclic shear of a viscoelastic layer of finite thickness  $H$ . The solution also describes torsional oscillations of a cylindrical sample of specified height, one of whose end is rigidly fastened. In this case, the shear stress at the fixed end depends linearly on the radius and, thus, is proportional to  $\sigma_{12}$ , and the linear velocity at the opposite end is proportional to  $v_2$ . Figure 3a gives the dependence for the Cosserat medium, and Fig. 3b gives the same dependence for a momentless

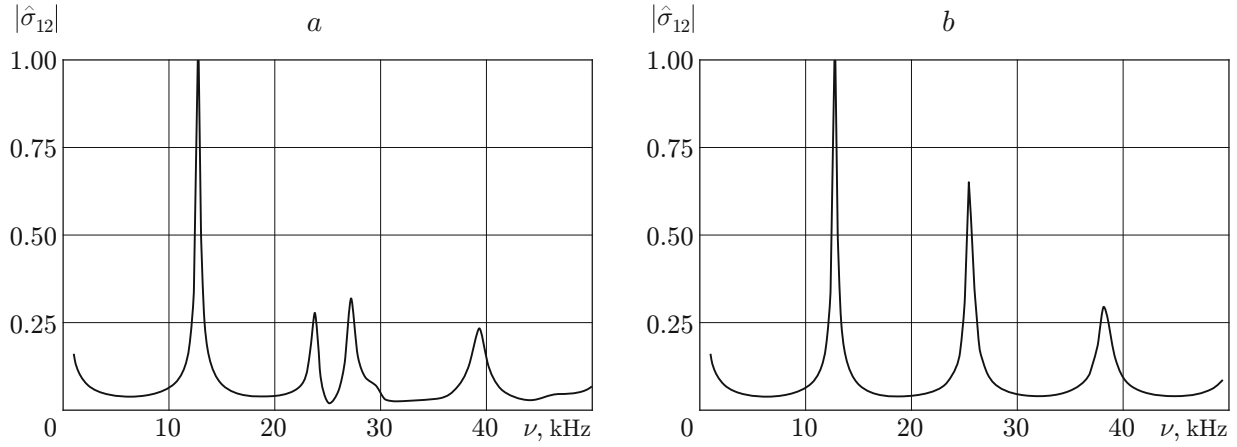


Fig. 3. Spectral dependences of shear stress for heavy oil in rock: (a) Cosserat medium; (b) momentless viscoelastic medium.

viscoelastic medium. The same dependences for ideal inviscid media have a system of resonant peaks with infinite amplitudes. Viscosity was used as a smoothing parameter. The shear process was described by Eqs. (2.3) in which, according to the Boltzmann viscoelasticity theory, the products of the parameters of the medium and the kinematic characteristics of deformation were replaced with convolutions of the relaxation kernels corresponding to these parameters on the same characteristics. The boundary conditions of the problem were given by

$$v_2 \Big|_{x_1=0} = v_0 e^{2\pi i \nu t}, \quad \omega_3 \Big|_{x_1=0} = 0, \quad v_2 \Big|_{x_1=H} = \omega_3 \Big|_{x_1=H} = 0 \quad (3.2)$$

(the  $x_1$  axis is directed inside the layer). System (2.3) was solved using the spectral method: after a Fourier transformation, system (2.3) led to the system of ordinary differential equations for the amplitudes

$$\begin{aligned} 4\pi^2 \nu^2 \rho \hat{v}_2 + (\hat{\mu} + \hat{\alpha}) \hat{v}_{2,11} - 2\hat{\alpha} \hat{\omega}_{3,1} &= 0, \\ 4(\pi^2 \nu^2 j - \hat{\alpha}) \hat{\omega}_3 + (\hat{\gamma} + \hat{\varepsilon}) \hat{\omega}_{3,11} + 2\hat{\alpha} \hat{v}_{2,1} &= 0, \end{aligned} \quad (3.3)$$

whose solution was constructed in explicit form taking into account boundary conditions (3.2). The shear stress amplitude was determined through the solution (3.3) using the formula

$$2\pi i \nu \hat{\sigma}_{12} = (\hat{\mu} + \hat{\alpha}) \hat{v}_{2,1} - 2\hat{\alpha} \hat{\omega}_3.$$

To check the reliability of the results, we performed a numerical solution of the problem based on the approximating (3.3) spectral-difference scheme

$$\begin{aligned} 4\pi^2 \nu^2 \rho \hat{v}_2^k + (\mu + \alpha) \frac{\hat{v}_2^{k+1} - 2\hat{v}_2^k + \hat{v}_2^{k-1}}{h^2} - 2\alpha \frac{\hat{\omega}_3^k - \hat{\omega}_3^{k-1}}{h} &= 0, \\ 4(\pi^2 \nu^2 j - \hat{\alpha}) \hat{\omega}_3^k + (\gamma + \varepsilon) \frac{\hat{\omega}_3^{k+1} - 2\hat{\omega}_3^k + \hat{\omega}_3^{k-1}}{h^2} + 2\alpha \frac{\hat{v}_2^{k+1} - \hat{v}_2^k}{h} &= 0, \end{aligned} \quad (3.4)$$

where  $h = H/N$  is the mesh step;  $k = 1, \dots, N-1$ . The calculations were performed by the matrix sweep method, and the results obtained on fine meshes were almost the same.

In the calculations, the phenomenological parameters of the medium were chosen from experimental data [8] for heavy oil in rock at a fairly low temperature at which the material was in the solid phase ( $\rho = 1114 \text{ kg/m}^3$ ,  $j = 0.01 \text{ kg/m}$ ,  $\mu = 966$ ,  $\alpha = 52.2 \text{ MPa}$ ,  $\gamma + \varepsilon = 12.51 \text{ N}$ , and  $H = 36.4 \text{ mm}$ ). In the calculations, the Kelvin-Voigt theory was used, according to which the complex moduli are linear functions of frequency, in particular,  $\hat{\mu} = \mu + 2\pi i \nu \mu'$ . The imaginary parts were chosen so as to achieve the required smoothing of the solution.

A comparison of Figs. 3a and 3b shows that a moment medium has an additional resonant frequency of 23 kHz, close to the frequency of rotational motion of the particles, which does not depend on the layer thickness. This is supported by data of a large number of numerical experiments for various thicknesses. It is found that a

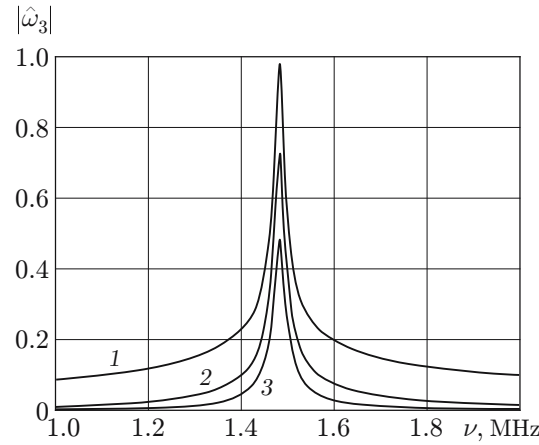


Fig. 4. Spectral dependence of angular velocity for synthetic polyurethane at  $H = 10$  cm and various distances from the surface of the layer:  $x_1 = 0$  (1),  $H/4$  (2), and  $H/2$  (3).

change in the thickness of the layer  $H$  leads to a displacement of the periodic system of the fundamental resonant frequencies approximately equal to  $\nu_k = kc_s/(2H)$  ( $k = 1, 2, \dots$ ), with the peak corresponding to the frequency  $\nu_*$  remaining motionless.

Similar calculations for foam polyurethane did not show a significant (compared to the fundamental frequencies) peak at the resonant frequency, which for this material has the same order of magnitude as for heavy oil. This is due to significantly lower moment characteristics expressed by the values of the parameter  $j$  and  $\alpha$ . It is found that in materials with low moment characteristics, the resonance of rotational motion of particles can be excited, for example, by periodically changing the rotational moment on the boundary of the layer. Figure 4 gives spectral curves for synthetic polyurethane with parameters  $\rho = 590$  kg/m<sup>3</sup>,  $j = 5.31 \cdot 10^{-6}$  kg/m,  $\lambda = 2.195$ ,  $\mu = 1.033$ ,  $\alpha = 0.115$  GPa,  $\beta = -2.34$ ,  $\gamma = 4.1$ ,  $\varepsilon = 0.13$  N (see [7]). The results were obtained by numerical solution using the spectral-difference method [see (3.4)] of system (3.3) subject to the boundary conditions

$$\sigma_{12}\Big|_{x_1=0} = 0, \quad m_{13}\Big|_{x_1=0} = m_0 e^{2\pi i \nu t}, \quad v_2\Big|_{x_1=H} = \omega_3\Big|_{x_1=H} = 0. \quad (3.5)$$

The above dependences were obtained for  $H = 10$  cm, but they are almost independent of the thickness of the layer. An analysis of Fig. 4 shows that, in the range studied, the angular velocity amplitude has a single resonant peak at a frequency  $\nu_* = 1.48$  MHz, whose height is adjusted by the imaginary part of the parameter  $\hat{\gamma} + \hat{\varepsilon}$  and decreases almost linearly with increasing depth.

Qualitatively, similar results in the problem with boundary conditions (3.5) were obtained in calculations performed for foam polyurethane and heavy oil. To support the numerical results analytically, we consider system (3.3) for  $\nu = \nu_*$  for an inviscid moment medium:

$$(4\alpha\rho/j)\hat{v}_2 + (\mu + \alpha)\hat{v}_{2,11} - 2\alpha\hat{\omega}_{3,1} = 0, \quad (\gamma + \varepsilon)\hat{\omega}_{3,11} + 2\alpha\hat{v}_{2,1} = 0. \quad (3.6)$$

For this system, the characteristic equation has a multiple root equal to zero with a multiplicity of two. The fundamental system of solutions consists of the vectors

$$\begin{pmatrix} -i(\gamma + \varepsilon)z \\ 2\alpha \end{pmatrix} e^{izx_1}, \quad \begin{pmatrix} i(\gamma + \varepsilon)z \\ 2\alpha \end{pmatrix} e^{-izx_1}, \quad \begin{pmatrix} 0 \\ 1 \end{pmatrix}, \quad \begin{pmatrix} j/(2\rho) \\ x_1 \end{pmatrix},$$

where  $z = 2\sqrt{(\alpha\rho(\gamma + \varepsilon)/j + \alpha^2)/((\mu + \alpha)(\gamma + \varepsilon))}$ . The general solution of system (3.6) has the form

$$\hat{v}_2 = -i(\gamma + \varepsilon)z \left( A e^{izx_1} - B e^{-izx_1} \right) + jD/(2\rho),$$

$$\hat{\omega}_3 = 2\alpha \left( A e^{izx_1} + B e^{-izx_1} \right) + C + Dx_1.$$

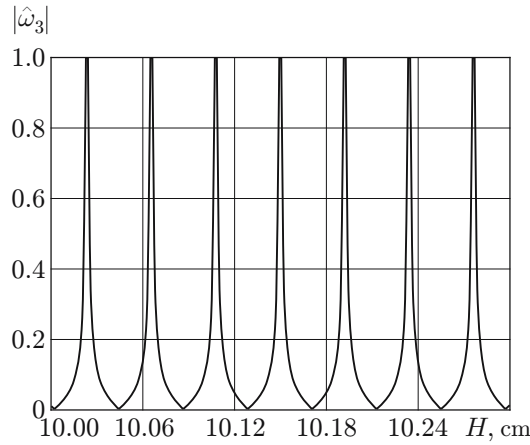


Fig. 5. Magnitude of angular velocity amplitude versus layer thickness.

By virtue of boundary conditions (3.5) on the surface  $x_1 = 0$ , the constants  $A$  and  $B$  are expressed in terms of  $C$  and  $D$ :

$$A + B = \frac{jC}{2\rho(\gamma + \varepsilon)}, \quad A - B = \frac{iD}{2\alpha z} + \frac{\pi\nu_* m_0}{\alpha z(\gamma + \varepsilon)}.$$

The boundary conditions on the surface  $x_1 = H$  lead to the system of equations

$$\begin{pmatrix} j\alpha z \sin(zH) & \rho(\gamma + \varepsilon) \cos(zH) + j\alpha \\ j\alpha z \cos(zH) + \rho z(\gamma + \varepsilon) & \rho(\gamma + \varepsilon)(zH - \sin(zH)) \end{pmatrix} \begin{pmatrix} C \\ D \end{pmatrix} = 2\pi i \rho \nu_* m_0 \begin{pmatrix} \cos(zH) \\ -\sin(zH) \end{pmatrix}, \quad (3.7)$$

which allows one to determine all constants. For  $x_1 = 0$ , the angular velocity amplitude is obtained from the formula

$$\hat{\omega}_3(0) = j\alpha C / (\rho(\gamma + \varepsilon)) + C.$$

From system (3.7), it follows that for large values of  $H$ , the constant  $D$  has the order of magnitude of  $1/H$  and  $C$  has the order of magnitude of  $\cot(zH)$ . Hence, the amplitude tends to infinity if  $zH$  is close to  $\pi k$  ( $k = 1, 2, \dots$ ).

Thus, in the problem with boundary conditions (3.5) ignoring the viscosity of the medium, the frequency  $\nu_*$  is resonant only for layers of strictly defined thickness. The increment in the thickness of the resonating layer  $\Delta H = \pi/z$  depends on the parameters of the material. For synthetic polyurethane, the value  $\Delta H = 0.42$  mm is comparable to the characteristic microstructure parameter  $r = 0.15$  mm. A curve of the amplitude  $\hat{\omega}_3(0)$  versus layer thickness is given in Fig. 5. It is evident that the asymptotic formula for the quantity  $\Delta H$  is satisfied with high accuracy.

**4. Calculations of Spatial Propagation of Waves.** In [3, 4], an algorithm for numerical implementation of system (1.2) on parallel architecture supercomputers is described and boundary symmetry conditions for the moment theory of elasticity for an isotropic medium are formulated which provide a reduction in calculation efforts due to cutoff of part of the computation domain. The algorithm is based on a second-order accuracy method of two-cyclic splitting over spatial variables and time. The one-dimensional systems of equations resulting from splitting are solved by means of an explicit monotonic predictor-corrector type essentially nonoscillatory (ENO) scheme which is a generalization of the Godunov discontinuity-decay scheme, using piecewise linear splines which are discontinuous on the boundaries of the cells. The splines are constructed by a special limiting-reconstruction procedure, which improves the accuracy of the numerical solution. The computation scheme obtained in this manner has the monotony property, and, in contrast to many simpler schemes, it can therefore be used to study generalized solutions in the problems of shock, pulse, and concentrated actions.

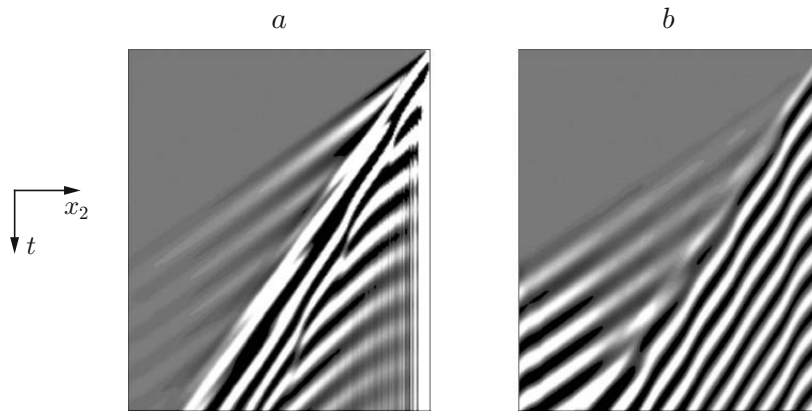


Fig. 6. Seismograms of incident waves in the case of pulse action (a) and periodic action (b).

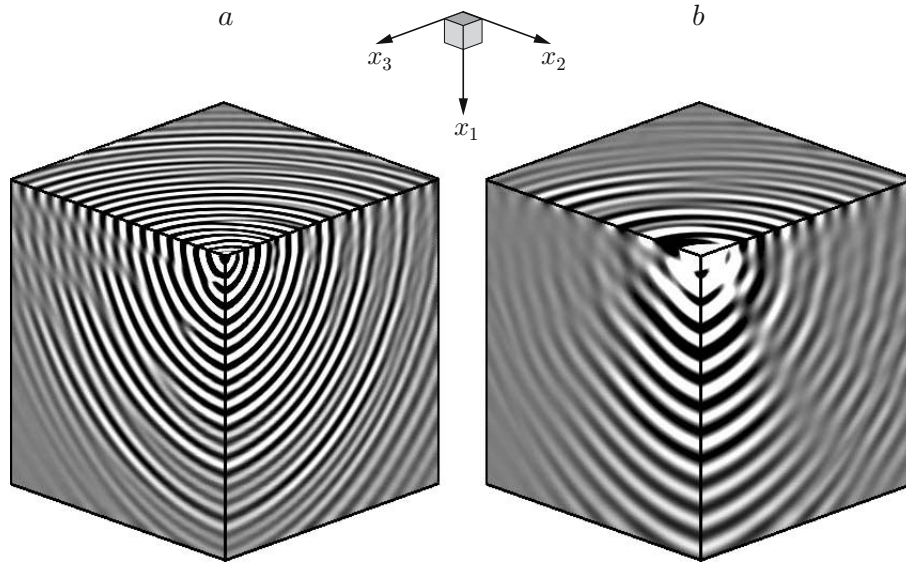


Fig. 7. Level surfaces of the angular velocity for nonresonant frequency (a) and resonant frequency (b).

Programming was performed using single-program multiple-data (SPMD) model in Fortran-95 with a message passing interface (MPI) library. The computation domain is distributed between the computation nodes according to the principle of uniform loading by means of one-, two-, or three-dimensional partitioning. The computations are unparallelized at the stage of splitting of the problem over spatial variables. The algorithm and complex of programs were tested by comparison of the calculation results with the exact solution of the two-dimensional problem of Rayleigh surface wave propagating in a Cosserat [9] medium and with the exact solutions describing one-dimensional motion of a medium with plane waves. The calculation results for natural oscillations in a moment medium in a two-dimensional formulation based on the proposed algorithm are given in [3]. The results of numerical solution of the spatial Lamb problem of instantaneous action of point forces and moments on the surface of a half-space are presented in [4]. Below, we give the results of numerical solution of the problem of the action of a point rotational moment  $m_{12} = -m_0\delta(x)\sin(2\pi\nu_*t)$  which varies periodically in time at a frequency equal to the resonant frequency.

In view of the symmetry conditions, the computation domain is a 1/4 half-space. In reality, the calculations were performed on a cube of synthetic polyurethane with a side 1 cm long. In the calculations, we used a uniform difference mesh with  $200 \times 200 \times 200$  cells. On rougher meshes, it is impossible to perform calculations with



admissible accuracy since the cell size becomes comparable to the microstructure parameter. On the artificially introduced sides of the cube, we specified symmetry conditions [4] and nonreflecting boundary conditions which modeled unobstructed passage of waves. The calculations were performed on the MBC-1000 cluster of the Institute of Computational Modeling of the Siberian Division of the Russian Academy of Sciences. Each of 64 computation nodes solved part of the problem on a submesh with  $50 \times 50 \times 50$  cells. Calculation of 200 steps in time requires approximately 10 h machine time. Figure 6a gives seismograms of the rotation angle of particles around a horizontal axis along the horizontal line through the point of loading for the Lamb problem and the problem of periodic action with resonant frequency  $\nu_*$ . The results are processed in the SeisView computer system. A comparison of the seismograms for the number of oscillations shows that the corresponding wavelengths almost coincide.

The level surfaces of the angular velocity  $\omega_2$  for a nonresonant frequency  $\nu = 1.5\nu_*$  and the resonant frequency  $\nu_*$  are shown in Figs. 7a and 7b, respectively. The calculations show that, at the frequency of external action  $\nu = \nu_*$ , the amplitude increases in time and the oscillations attenuate slowly with increasing distances, which is typical of acoustic resonance.

The calculations results can form a methodical basis for designing experiments to determine the phenomenological parameters of Cosserat continuum (a problem which has not been solved so far).

This work was supported by the Russian Foundation for Basic Research (Grant No. 08-01-00148), the Complex Program of Basic Research of the Presidium of the Russian Academy of Sciences No. 2 Intelligent information technologies, mathematical modeling, system analysis and automation, and the interdisciplinary Integration project of the Siberian Division of the Russian Academy of Sciences No. 40.

## REFERENCES

1. E. Cosserat and F. Cosserat, "Theorie des corps deformables," *Chwolson's Traité Physique*, Librairie Scientifique A. Hermann et Fils, Paris (1909), pp. 953–1173.
2. V. A. Pal'mov, "Governing equations of the theory of asymmetrical elasticity," *Prikl. Mat. Mekh.*, **28**, No. 3, 401–408 (1964).
3. O. V. Sadovskaya and V. M. Sadovskii, *Mathematical Modeling in Problems of Mechanics of Loose Media* [in Russian], Fizmatlit, Moscow 2008.
4. O. V. Sadovskaya, "Numerical solution of spatial dynamic problems of the moment theory of elasticity with boundary symmetry conditions," *Zh. Vychisl. Mat. Mat. Fiz.*, **49**, No. 2, 313–322 (2009).
5. S. K. Godunov, *Equations of Mathematical Physics* [in Russian], Nauka, Moscow (1979).
6. O. V. Sadovskaya and V. M. Sadovsky, "Numerical analysis of elastic waves propagation in Cosserat continuum," in: *Proc. of the 8th Int. Conf. on Mathematical and Numerical Aspects of Wave Propagation (Waves 2007)* (Univ. of Reading, England, 23–27 July, 2007), INRIA, Paris (2007), pp. 327–329.
7. R. Lakes, "Experimental methods for study of Cosserat elastic solids and other generalized elastic continua," in: H. Mühlhaus and J. Wiley (ed.), *Continuum Models for Materials with Micro-Structure*, Chapter 1, Wiley and Sons, New York (1995), pp. 1–22.
8. J. Behura, M. Batzle, R. Hofmann, and J. Dorgan, "Heavy oils: Their shear story," *Geophys.*, **72**, No. 5, E175–E183 (2007).
9. M. A. Kulseh, V. P. Matveenko, and I. N. Shardakov, "Propagation of elastic surface waves in a Cosserat medium," *Dokl. Ross. Akad. Nauk*, **405**, No. 2, 196–198 (2006).